ELSEVIER

Journal of Nuclear Materials 250 (1997) 63–74

journal of nuclear materials

Spent LWR fuel dry storage in large transport and storage casks after extended burnup

Harry Spilker [a], Martin Peehs [b,*], Hans-Peter Dyck [b], Guenter Kaspar [b], Klaus Nissen [b]

[a] *Gesellschaft für Nuklearbehälter, Essen, Germany*

[b] *Siemens AG, Power Generation Group (KWU), P.O. Box 3220, 91050 Erlangen, Germany*

Received 2 December 1996; accepted 14 June 1997

Abstract

Dry spent LWR fuel storage is licensed for single fuel assemblies with rod burnup to 65 GWd/tHM. This allows dry spent fuel storage of reloads with a batch average up to 55 GWd/tHM. The leading defect mechanism for spent fuel rods in dry storage is hoop strain. Fuel rod degradation can be prevented by limiting creep. Post-pile creep of fuel rod cladding can be described conservatively by the creep of unirradiated cladding. In order to extend the database, internally pressurized creep samples were investigated for time intervals up to 10 000 h. Test temperatures were between 250 and 400°C, and the hoop stresses applied ranged from 80 to 150 N/mm^2. The resulting data were described mathematically by an interpolation formula. Based on the fuel assemblies end-of-life data the maximum CASTOR V cask storage temperature was calculated to be between 348°C and 358°C at the beginning. © 1997 Elsevier Science B.V.

1. Introduction

The total amount of spent fuel accumulated worldwide at the end of 1994 was over 155 000 tHM. Of this, about 60% was stored in storage facilities awaiting either reprocessing or final disposal [1]. The projected cumulative amount of spent fuel generated by the year 2010 is expected to reach 300 000 tHM. Assuming that part of this spent fuel will be reprocessed, the amount to requiring storage is projected to be about 200 000 tHM. Therefore, interim storage will be the primary spent fuel management option worldwide. In Germany, we find that after the adoption of the *Artikelgesetz* (energy policy amendments to the Atomic Energy Act), long-term interim storage together with direct disposal and reprocessing, practiced in parallel, form the two options for the back end of the fuel cycle strategy [2]. The dry storage technology selected, developed and implemented in Germany is storage of spent fuel assemblies in CASTOR-type [3] transport and storage casks.

In order to reduce the amounts of spent fuel circulating within the nuclear fuel cycle, fuel assembly burnup has been increased considerably in Germany in the course of the last two decades to the extent that average batch burnups of 55 GWd/tHM will be achieved in the near future [4]. CASTOR casks type I and II are licensed for fuel assembly burnup of < 40 GWd/tHM. In order to meet with increasing burnup requirements and to achieve, for economic reasons, larger amounts of spent fuel in a single cask, the CASTOR V cask was developed which can accommodate 19 pressurized water reactor (PWR) fuel assemblies or 52 boiling water reactor (BWR) fuel assemblies. The CASTOR V cask series is designed for spent fuel assemblies with thermal and nuclear source terms typically for fuel assemblies with a rod burnup up to 65 GWd/tHM. Therefore, suitable combinations of fuel assemblies from a reload batch with an average burnup of 55 GWd/tHM can be loaded into the CASTOR V cask even if individual fuel assemblies from such reloads have higher fuel assembly burnup. However, fuel assemblies in the burnup range under consideration — e.g., MOX fuel assemblies — might even limit cask capacity [5] due to the higher nuclear and thermal source terms in comparison to uranium fuel assemblies.

* Corresponding author.

PII S0022-3115(97)00209-2

The CASTOR V cask, like all other CASTOR cask types, is designed by applying the double barrier principle in order to safely and reliably retain all activity under normal and off-normal conditions. Licensing requires that no systematic fuel failure occur in the cask under the given storage conditions. A detailed materials research program on Zircaloy-type cladding material was therefore performed to support licensing of the CASTOR V cask.

2. Experience with dry storage

2.1. International experience

Dry storage has become a mature technology [6,7]. Canada has the largest amount of spent fuel stored under dry conditions [8]. The yearly quantity in Canada amounts to 25 000 spent fuel assemblies. Dry spent fuel storage is also becoming more and more significant in the United States as the volume of spent fuel will exhaust the capacity of wet spent fuel storage ponds in the course of time. In Japan, a dry storage cask storage facility began operation in 1995 [6,9]. Russia is planning to construct dry storage facilities for RBMK nuclear power plants [10]. The United Kingdom [11] and France [7] are employing dry storage methods as well as South Korea [12] and Germany.

Most countries use helium as the storage atmosphere, although both air and helium are used in Canada, while South Korea uses an air atmosphere only. The best worldwide summary of lightwater reactor-related temperature limit determination for inert dry storage of spent fuel assemblies was published by EPRI [13]: cladding creep from internal gas overpressure constitutes the rate-determining degradation and failure mechanism for setting maximum allowable storage temperature limits in dry inert storage. If creep were allowed to proceed to rupture, the fracture mode would most likely be of a pinhole type. Nevertheless, it is desirable to avoid any degradation. This can be accomplished by confining the creep degradation mechanism to its primary and early secondary stages. If it can be shown that creep strain never exceeds that critical strain domain during inert *dry storage*, tertiary creep and subsequent fuel rod defection can be ruled out. This approach is commensurate with standard creep engineering practices and relies on the availability of the following:

- a database of cladding creep test results under internal pressurization conditions,
- a correlation which allows prediction of post-pile creep from creep of unirradiated material,

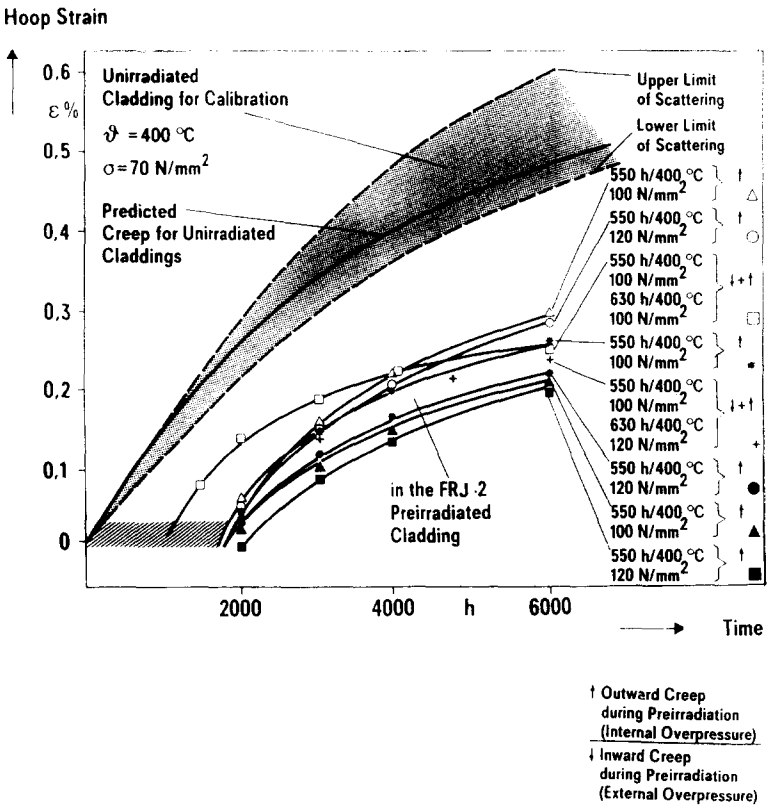

Fig. 1. Comparison of creep strain of unirradiated and irradiated Zry-4 cladding.

Table 1
Scope of spent LWR fuel assembly dry storage in Germany

Type	Fuel assembly type/power plant	No. of fuel assemblies	Time in dry storage
CASTOR Ic	BWR/Würgassen	16	24 months
CASTOR Ib	PWR/Stade	4	24 months
CASTOR Ia	PWR/Biblis	4	30 months
TN 1300	PWR/Biblis	12	1 week
CASTOR Ib	PWR/Stade	4	1 week (operationally defective fuel)

- a database of the potential total strain of a fuel rod cladding under dry storage conditions,
- a numerical model to predict creep strain during dry storage.

2.2. Experience in Germany

Systematic studies had been performed in Germany in preparation for dry storage of spent lightwater reactor (LWR) fuel. In a first step, the leading failure mechanism was identified [14]. Based on the result that creep is the leading defect mechanism, an approach to describe the post-pile creep by the creep of unirradiated materials was developed and validated [15]. Fig. 1 shows the hoop strain results from unirradiated and irradiated creep samples. The creep tests for both materials were performed simultaneously in the same test device. The results from the post-pile creep test program were used to predict the dry storage performance of spent LWR fuel [16].

Validation [17] was performed by using the dry storage CASTOR demonstration test program [18]. The scope of this program is described in Table 1.

The main results of all these investigations can be summarized as follows.

(1) Creep is the leading failure mechanism.

(2) Creep equations derived from unirradiated cladding describe conservatively post-pile creep of fuel assemblies in dry storage.

(3) For burnups of < 40 GWd/tHM, no fuel rod defection will occur if strain is limited to 1% during storage.

Based upon the experimentally verified results, the CASTOR I and CASTOR II casks have been licensed for transport and storage of spent fuel assemblies with burnups less than or equal to 40 GWd/tHM. These casks can be used for storage at the Ahaus and Gorleben repositories, two storage facilities being licensed for extended interim dry storage of spent nuclear fuel.

3. Castor cask technology

The main type of cask built by the Gesellschaft für Nuklearbehälter (GNB) is the CASTOR model made of ductile cast iron. All design criteria, including all testing in accordance with IAEA regulations for a Type B(U) F package as well as the acceptance criteria for the German storage sites, are fulfilled by the CASTOR V cask family. A state-of-the-art and high-capacity design, CASTOR V

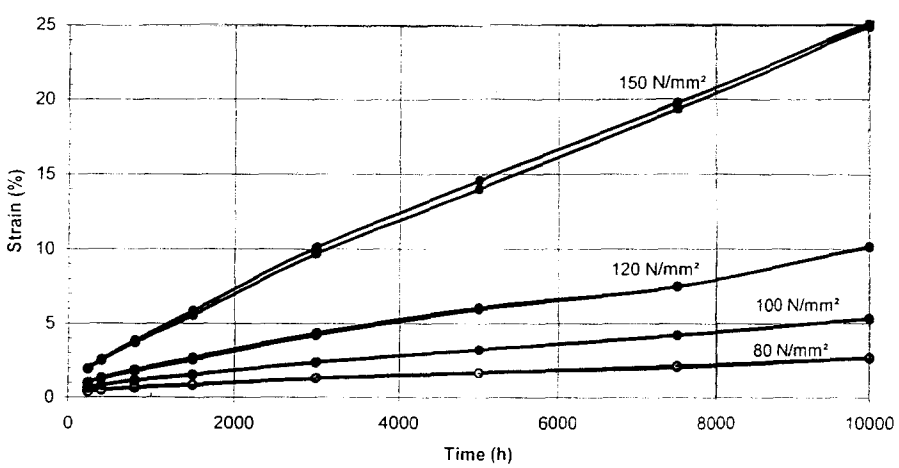

Fig. 2. Creep strain of cladding type I at 375°C.

has been developed for transport and long-term interim storage of either 19 PWR/21 PWR or 52 BWR spent fuel assemblies. The mass of heavy metal per fuel assembly is 560 kg for the CASTOR V/19 (PWR) and 187 kg for the CASTOR V/52 (BWR). Maximum allowable heating per cask is 38 kW.

The CASTOR casks are designed with machined 60 mm high radial fins on the cylindrical outer surface of the cask to achieve better passive heat removal. The primary and the secondary lids are made of stainless steel and have separate metallic and elastomer seals to secure leaktightness. Both lids are secured by bolts. Four trunnions are provided for handling operations, two each at the top and bottom ends of the cask. The trunnions are designed to the German KTA nuclear safety standard 3905.

Moderator rods are provided within the cask wall as well as moderator plates at the top and bottom lids of the cask for a better neutron shielding. The moderator material is polyethylene.

A fuel basket made of partly borated stainless steel is located in the cask cavity. The basket provides fuel assembly support, criticality control, and heat conduction paths. The cask body together with the lids and seals is used as the confinement system.

Table 2
Strain acting on cladding samples of cladding type I

Temp. (°C)	Diameter (mm)	Stress (MPa)	Strain (%) after ... h							
			240	400	800	1500	3000	5000	7500	10000
250	10.75	80	0.06	0.06	0.07	0.07	0.06	0.07	0.08	0.13
		80	0.06	0.06	0.07	0.07	0.06	0.06	0.11	0.13
		100	0.09	0.09	0.07	0.08	0.08	0.08	0.08	0.12
		100	0.06	0.08	0.09	0.07	0.07	0.07	0.08	0.16
		120	0.09	0.09	0.09	0.07	0.08	0.08	0.11	0.14
		120	0.08	0.08	0.09	0.09	0.07	0.09	0.11	0.15
		150	0.08	0.10	0.10	0.10	0.10	0.12	0.13	0.15
		150	0.10	0.11	0.11	0.11	0.11	0.14	0.17	0.18
300	10.73	80	0.06	0.08	0.08	0.11	0.09	0.11	0.19	0.23
		80	0.07	0.07	0.09	0.10	0.09	0.12	0.16	0.19
		100	0.11	0.11	0.12	0.14	0.13	0.16	0.20	0.29
		100	0.12	0.12	0.13	0.14	0.14	0.18	0.24	0.29
		120	0.12	0.12	0.16	0.18	0.19	0.21	0.27	0.33
		120	0.12	0.13	0.15	0.17	0.19	0.22	0.30	0.32
		150	0.15	0.15	0.21	0.22	0.26	0.32	0.42	0.45
		150	0.16	0.18	0.23	0.24	0.27	0.33	0.44	0.50
350	10.73	80	0.19	0.22	0.26	0.32	0.41	0.49	0.61	0.74
		80	0.20	0.23	0.27	0.32	0.41	0.49	0.65	0.74
		100	0.29	0.31	0.40	0.48	0.63	0.81	1.04	1.24
		100	0.26	0.31	0.39	0.48	0.63	0.81	0.98	1.17
		120	0.35	0.43	0.54	0.71	0.94	1.22	1.55	1.84
		120	0.37	0.43	0.57	0.73	0.95	1.23	1.58	1.86
		150	0.59	0.72	0.96	1.27	1.79	2.40	3.20	3.78
		150	0.59	0.71	0.96	1.26	*1.67*	*2.08*	*2.41*	*2.55*
375	10.74	80	0.43	0.50	0.66	0.88	1.29	1.69	2.05	2.71
		80	0.39	0.48	0.64	0.84	1.30	1.66	2.14	2.67
		100	0.67	0.80	1.13	1.55	2.39	3.24	4.24	5.33
		100	0.66	0.80	1.13	1.54	2.37	3.24	4.21	5.3
		120	1.00	1.29	1.85	2.69	4.36	6.07	7.47	10.17
		120	0.98	1.27	1.78	2.57	4.23	5.96	7.47	10.13
		150	1.96	2.55	3.85	5.85	10.08	14.58	19.75	25.13
		150	1.92	2.50	3.71	5.56	9.68	14.02	19.33	24.85
400	10.74	80	0.63	0.84	1.23	1.83	2.79	4.05	5.58	7.32
		80	0.66	0.87	1.31	1.85	2.78	4.00	5.47	7.10
		100	1.11	1.45	2.25	3.38	5.41	8.06	11.24	14.52
		100	1.15	1.54	2.35	3.48	5.42	8.23	11.38	14.86
		120	1.95	2.62	3.91	5.84	*8.43*	*9.97*		
		120	1.89	2.54	3.88	6.05	10.12	15.34	22.09	28.81
		150	3.88	5.35	8.38	12.91	23.57	37.88	58.24	87.45
		150	3.96	5.34	8.39	12.90	23.09	38.12	58.41	83.20

The cask body consists of a thick-walled, cylindrical cask body made in one piece of ductile cast iron. This material exhibits sufficient ductility and strength. The inner surfaces of the cask are nickel coated; the outer surfaces are provided with an easily decontaminating protective paint coating of epoxy resin base.

4. The experimental program

4.1. The experimental approach

The creep samples were each manufactured as an individually closed pressurized test sample. Internal gas pressure was controlled such that the sample is subjected to the predetermined hoop stress at the test temperature. The length of the samples was equal to $10\times$ rod diameter. Helium was used as the internal pressurized atmosphere. Calculation of the hoop stress at test temperature was based on the ideal gas equations including an empirical correction factor $r_p(T)$. The hoop stress is calculated from the internal gas pressure by the following equation:

$$\sigma_\theta = d_i \times p/(d_a - d_i),$$

where p is the internal gas pressure, d_a the outside diameter and d_i the inside diameter.

Table 3
Strain acting on cladding samples of cladding types II through VI

Temp. (°C)	Type	Diameter (mm)	Stress (MPa)	Strain (%) after ... h							
				240	400	800	1500	3000	5000	7500	10000
375	II	12.26	80	0.13	0.16	0.23	0.30	0.46	0.65	0.89	1.13
			80	0.16	0.19	0.27	0.31	0.44	0.63	0.90	1.12
			100	0.26	0.30	0.41	0.59	0.92	1.30	1.67	2.09
			100	0.26	0.32	0.40	0.58	0.93	1.32	1.77	2.15
			120	0.49	0.61	0.90	1.27	2.06	2.89	3.81	4.52
			120	0.47	0.60	0.86	1.24	2.01	2.83	3.78	4.54
			150	1.47	1.89	2.90	4.35	6.97	9.46	12.26	14.28
			150	1.49	1.88	2.84	4.10	6.82	9.35	12.05	14.06
375	III	11.20	80	0.17	0.20	0.26	0.33	0.47	0.71	0.96	1.18
			80	0.17	0.15	0.24	0.31	0.44	0.69	0.93	1.15
			100	0.27	0.32	0.46	0.65	0.98	1.45	1.91	2.39
			100	0.26	0.32	0.43	0.66	0.96	1.50	1.96	2.40
			120	0.54	0.64	0.96	1.36	2.18	3.16	4.19	5.20
			120	0.51	0.62	0.91	1.31	2.07	3.2	4.20	5.11
			150	1.62	2.08	2.98	4.38	6.97	9.72	12.85	15.48
			150	1.59	2.02	2.86	4.24	6.73	9.88	12.84	15.55
375	IV	11.64	80	0.14	0.15	0.21	0.27	0.39	0.49	0.74	0.91
			80	0.11	0.14	0.18	0.25	0.38	0.46	0.71	0.87
			100	0.23	0.28	0.40	0.53	0.79	1.03	1.44	1.93
			100	0.19	0.24	0.34	0.45	0.70	0.90	1.31	1.67
			120	0.42	0.54	0.81	1.12	1.65	2.27	3.25	4.04
			120	0.39	0.51	0.74	1.02	1.59	2.06	2.96	3.78
			150	1.45	1.85	2.82	3.82	5.44	7.50	10.30	12.91
			150	1.27	1.61	2.35	3.21	4.92	6.37	8.58	10.86
375	V	9.60	80	0.14	0.16	0.21	0.27	0.41	0.56	0.81	1.00
			80	0.14	0.16	0.21	0.27	0.40	0.53	0.78	0.95
			100	0.25	0.29	0.42	0.55	0.79	1.13	1.60	2.06
			100	0.24	0.27	0.40	0.54	0.78	1.07	1.49	1.90
			120	0.55	0.65	0.94	1.29	1.72	2.55	3.57	4.37
			120	0.48	0.57	0.78	1.06	1.57	2.14	2.97	3.65
			150	1.72	2.04	2.88	3.86	5.43	7.80	10.54	12.79
			150	1.50	1.78	2.49	3.38	4.96	6.72	8.62	10.68
375	VI	9.62	80	0.11	0.12	0.18	0.22	0.32	0.48	0.66	0.84
			80	0.10	0.10	0.16	0.20	0.28	0.42	0.55	0.74
			100	0.17	0.20	0.27	0.36	0.52	0.78	1.06	1.37
			100	0.17	0.19	0.25	0.34	0.50	0.72	0.95	1.22
			120	0.28	0.33	0.47	0.62	0.94	1.34	1.79	2.34
			120	0.27	0.32	0.45	0.61	0.90	1.27	1.69	2.13
			150	0.67	0.80	1.12	1.58	2.17	3.19	4.22	5.29
			150	0.67	0.80	1.10	1.54	2.35	3.31	4.18	5.23

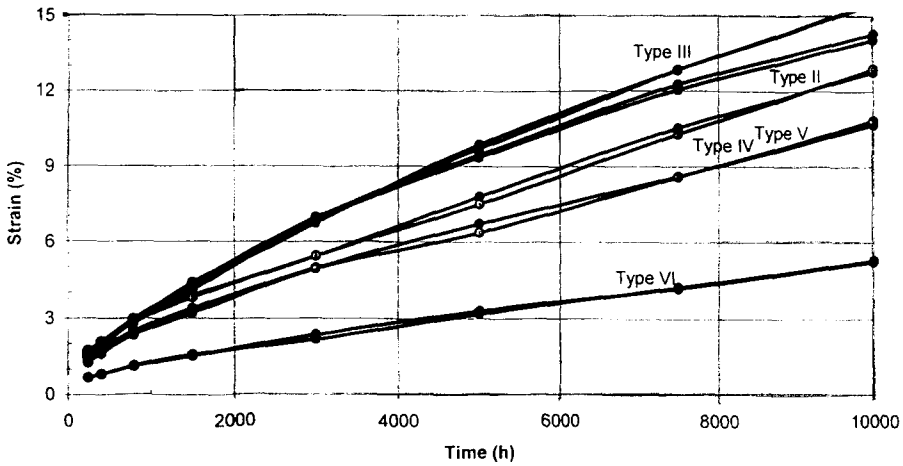

Fig. 3. Creep strain of cladding type II–VI at 150 N/mm^2 and 375°C.

The axial stress is half of the hoop stress. The axial strain therefore is small compared with the hoop strain. The internal volume increase is only due to the diameter growth. The tangential strain reduces the internal gas pressure by a factor of $(1+\varepsilon)^2$. The wall thickness is reduced by a factor of $(1+\varepsilon)$. The sample diameter is increased by the same amount. Insertion of these change

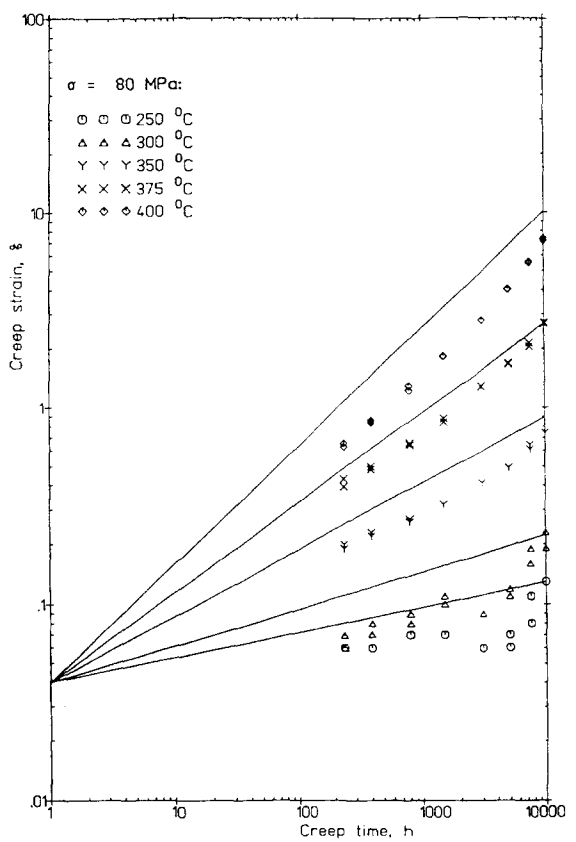

Fig. 4. Experimental creep data and calculated values using the developed mathematical creep equation: Hoop stress = 80 N/mm^2.

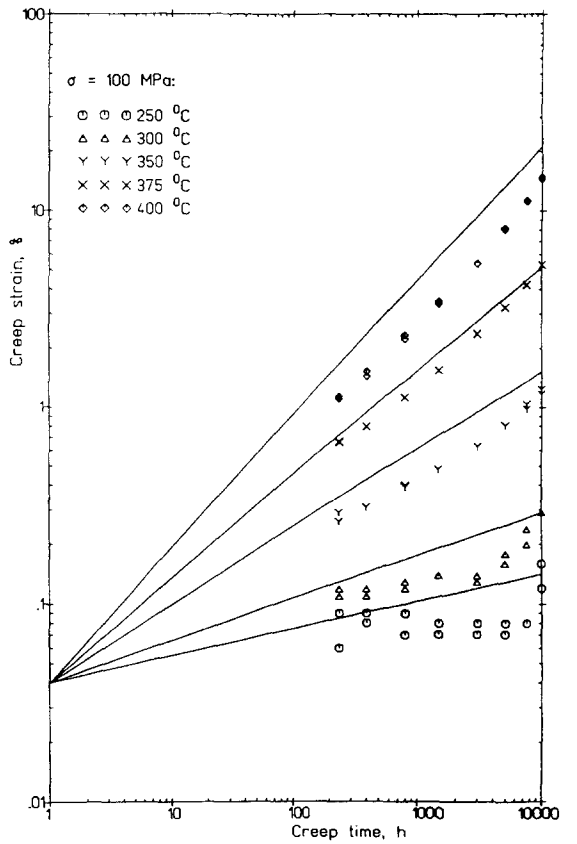

Fig. 5. Experimental creep data and calculated values using the developed mathematical creep equation: Hoop stress = 100 N/mm^2

Table 4
Scope of strain analysis for CASTOR V casks loaded with spent LWR fuel assemblies

Case	1	2	3	4	Measuring unit
Cladding	cladding displaying faster creep rate		cladding displaying slower creep rate		
Rod burnup	55	55	55	55	GWd/tHM
Fuel	UO_2	UO_2/PuO_2	UO_2	UO_2/PuO_2	
Pond storage	5.6	6.5	5.6	6.5	years
Decay heat cask	32.2	37.5	32.3	37.5	kW begin of storage
Fuel rod hot spot temp.	348	357	348	357	°C
Storage period	40	40	40	40	years

values into the equation to calculate hoop stress reveals that the hoop stress remains constant throughout the entire test. The samples were removed from the furnace in order to perform the geometrical measurements of the test samples. Measurements were taken at ambient temperature. The accuracy of these dimensional checks is ± 3 μm. The accuracy of the internal gas pressure is ± 0.2 bar, resulting in a scatter of the hoop stress of about ± 2.5 N/mm.

4.2. Scope of testing

One main type of cladding selected (test type I) which has a nominal diameter of 10.75 mm was tested applying hoop stresses of 80, 100, 120 and 150 N/mm^2. The test temperatures were 250, 300, 350, 375 and 400°C, and test duration was 10 000 h. Intermediate measurements were performed after 240, 400, 800, 1500, 3000, 5000 and 10 000 h. Each sample is characterized at each time step by an averaged value of all measurements taken.

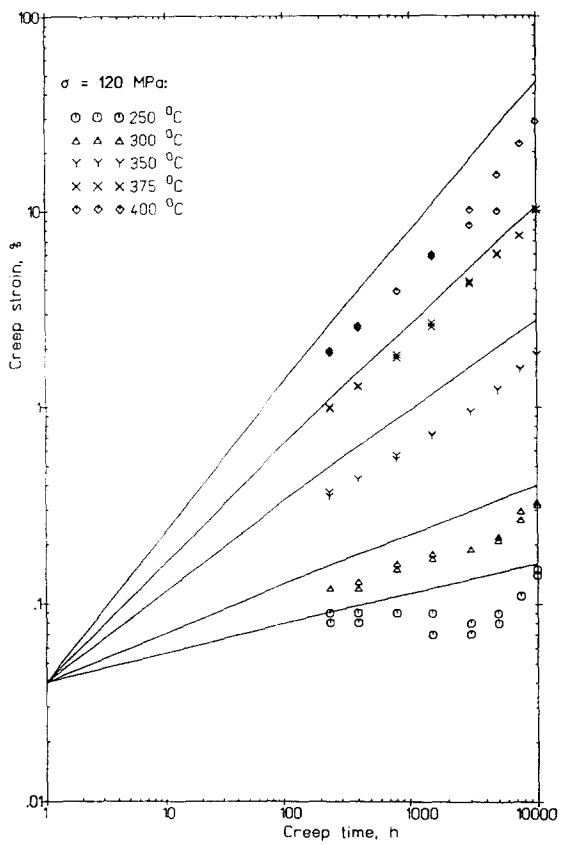

Fig. 6. Experimental creep data and calculated values using the developed mathematical creep equation: Hoop stress = 120 N/mm^2

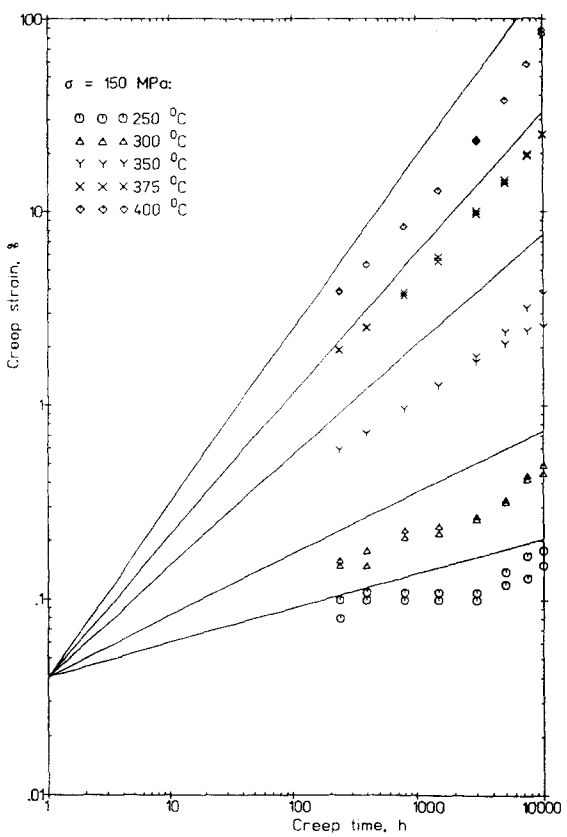

Fig. 7. Experimental creep data and calculated values using the developed mathematical creep equation: Hoop stress = 150 N/mm^2.

Five further types of cladding, numbered II through VI, were tested additionally using a reduced testing program comprising hoop stresses of 80, 100, 120, and 150 N/mm^2 at only one temperature level (375°C).

4.3. Results of experimental testing

The measured strain data are compiled in Tables 2 and 3. Two test samples began to leak during the test. The measured data from these two samples are shown in italics. These leaking samples were removed from testing after 5000 h.

The test results given in Tables 3 and 4 are presented in the following figures. Figs. 2 and 3 compare the creep strain from cladding type I with that of cladding types II to V at the test temperature of 375°C and various stresses. The creep strain response under a given set of stresses differs significantly for the zirconium alloy Zircaloy 4 depending on the composition and metallurgical state of the cladding type considered.

5. Discussion and application experimental results

5.1. Post-pile creep equation

With reference to our earlier results, the post-pile creep can be described conservatively by the creep of unirradiated material. In order to elaborate the creep equation we selected the fastest creeping cladding type I for the reference equation. In addition, all measured data points should be equal to or less than the calculated prediction. This approach assures that the post-pile creep of any spent fuel rods with Zircaloy cladding — including recently used low-tin Zircaloy-type claddings — will be described conservatively.

Creep strain of cladding type I can be conservatively approximated by the following equation:

$$\varepsilon = At^m \text{ or } \log \varepsilon = \log A + m \log t,$$

where ε is the creep strain in %, A is the initial strain of 0.04% and t is the time in h.

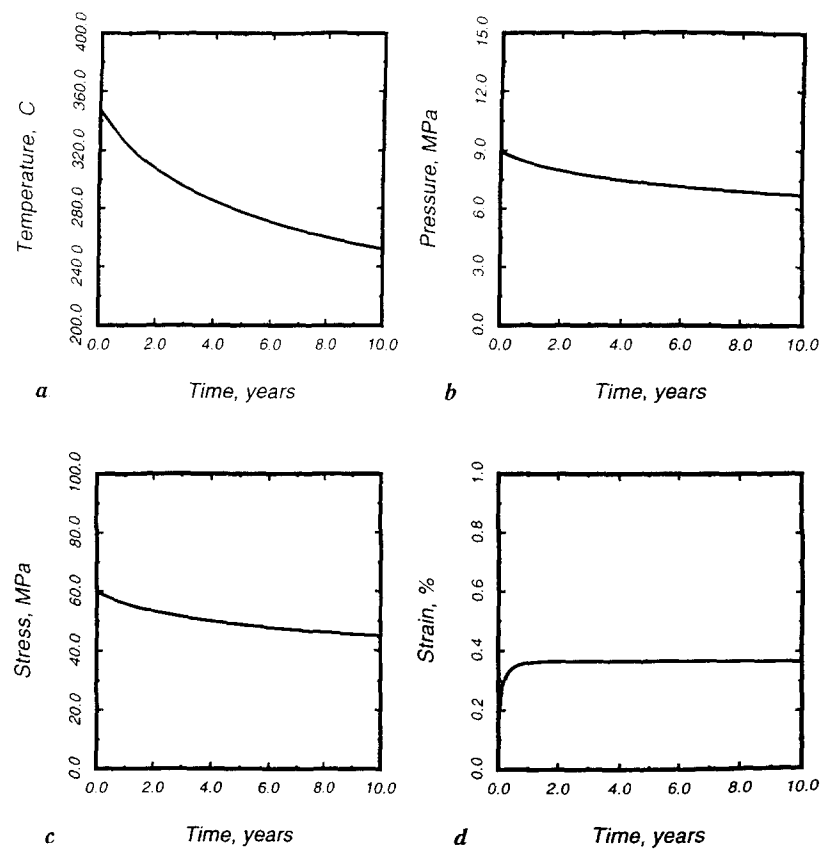

Fig. 8. Spent fuel storage performance prediction of a fuel rod with a burn-up of 55 GWd/tHM, UO_2-fuel pellet and fast creeping cladding.

Table 5
Conditions at begin of dry storage for cases 1–4

Cladding	Lower temperature	Higher temperature
Cladding displaying faster creep rate	348°C, $\sigma_{hoop} = 60$ N/mm^2, case 1	357°C, $\sigma_{hoop} = 60$ N/mm^2, case 2
Cladding displaying slower creep rate (stronger cladding)	348°C, $\sigma_{hoop} = 80$ N/mm^2, case 3	357°C, $\sigma_{hoop} = 80$ N/mm^2, case 4

The time exponent m can be described as a function of stress and temperature:

$$m = c_1 + c_2 T_f + c_3 T_f^2 + \ldots + c_{11} T_f^{10},$$

valid for 100°C $< T <$ 400°C and 80 MPa $< \sigma <$ 150 MPa, where

$$T_f = T + (\sigma - 80) \times 45/70$$

and $c_1 = 0.361705 \times 10^{-13}$, $c_2 = 0.500028 \times 10^{-3}$, $c_3 = -0.555901 \times 10^{-6}$, $c_4 = 0.715481 \times 10^{-7}$, $c_5 = -0.181897 \times 10^{-8}$, $c_6 = 0.207254 \times 10^{-10}$, $c_7 = -0.126131 \times 10^{-12}$, $c_8 = 0.433320 \times 10^{-15}$, $c_9 = -0.835848 \times 10^{-18}$, $c_{10} = 0.842689 \times 10^{-21}$, $c_{11} = -0.345181 \times 10^{-24}$.

For temperature values lower than the experimental range a nearly linear decrease of the time exponent to the value $m = 0$ at 0°C is included in the polynomial. This is a conservative assumption since it is well known that thermal creep strain decreases very quickly with decreasing temperature. Figs. 4–7 show how the interpolation equation conservatively describes the experimental data from cladding type I. It can also be seen that in all cases the mathematical equation overestimates somewhat the strain of the test samples.

6. Spent fuel rod strain in a loaded CASTOR V cask

The following CASTOR V/19 cask loadings are considered:

– 19 LWR fuel assemblies with UO_2 as nuclear fuel having a maximum rod burnup of 55 GWd/tHM, or

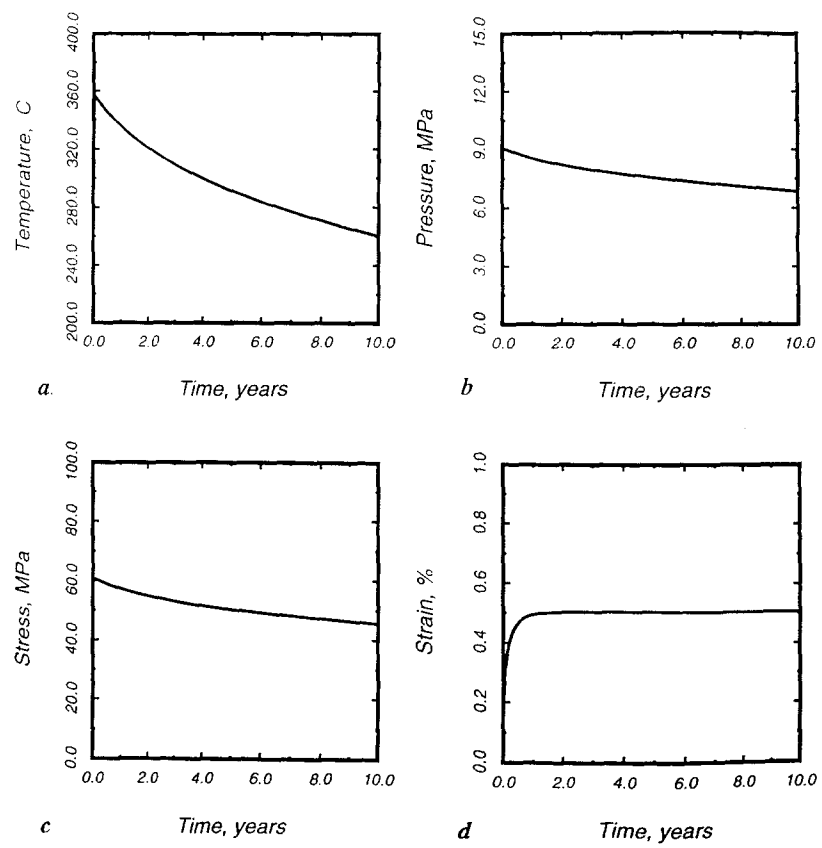

Fig. 9. Spent fuel storage performance prediction of a fuel rod with a burn-up of 55 GWd/tHM, MOX-fuel pellet and fast creeping cladding.

Table 6
Hoop strain in cases 1–4 after 40 years of dry storage

Cladding	Lower temperature	Higher temperature
Cladding displaying faster creep rate	0.37%	0.51%
Cladding displaying slower creep rate (stronger cladding)	0.52%	0.77%

– 15 LWR fuel assemblies with UO_2 as nuclear fuel and 4 LWR fuel assemblies with UO_2/PuO_2 as nuclear fuel, both having a maximum rod burnup of 55 GWd/HM.

Additionally, we looked at 2 types of fuel rod claddings to assess the influence of different cladding materials. Table 4 presents the scope of assessment.

Siemens-PCA-2 is an example of a relatively fast creeping cladding whereas the Siemens-DUPLEX cladding represents a relative strong cladding. In calculating the end-of-life (EOL) for reactor operation, the differing inservice behaviors of these cladding types have been considered. Due to the downwards creep under the external coolant pressure, fast creeping cladding contacts the oxide fuel earlier than strong cladding. As a result of the earlier closed fuel cladding gap, the fuel temperature and consequently the fission gas release is less than in the case of the stronger cladding. Therefore, at the begin of dry storage the internal fuel rod pressure in cases 1 and 2 is lower than in cases 3 and 4. The initial conditions for dry storage of the four cases considered are compiled in Table 5.

The results of calculations for cases 1 through 4 are presented in Figs. 8–11 and in Table 6. These figures show the following:

(a) hot spot fuel rod temperature as a function of time,

(b) internal fuel rod pressure as a function of time,

(c) hot spot hoop stress at mid-wall cladding calculated by a thick wall cylinder [19],

(d) hoop strain as a function of time.

Since it is generally accepted that spent Zircaloy-type cladding can withstand under dry storage conditions, at least 1% hoop strain, the results presented indicate that under the conditions considered spent LWR fuel up to a

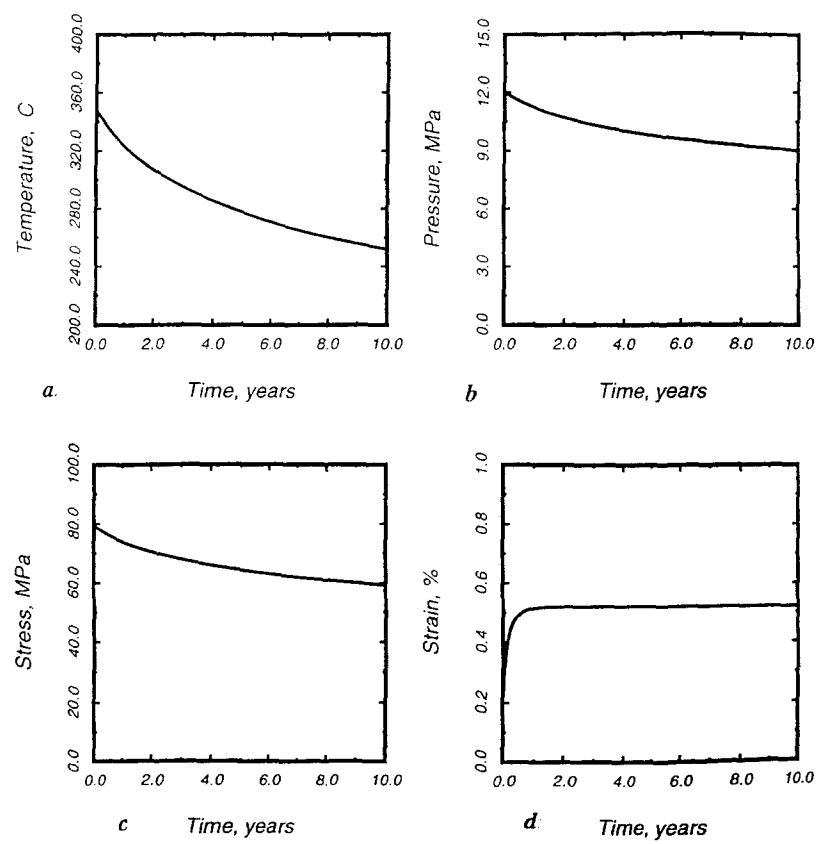

Fig. 10. Spent fuel storage performance prediction of a fuel rod with a burn-up of 55 GWd/tHM, UO_2-fuel pellet and strong cladding.

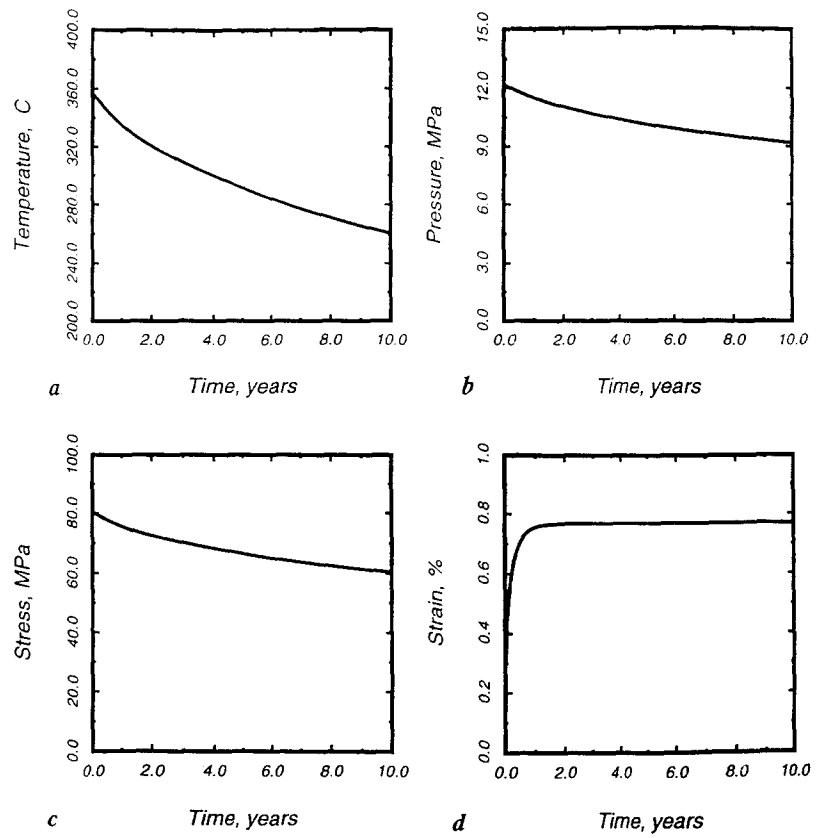

Fig. 11. Spent fuel storage performance prediction of a fuel rod with a burn-up of 55 GWd/tHM, MOX-fuel pellet and strong cladding.

fuel rod average burnup of 55 GWd/tHM can be stored free of fuel assembly defects for time periods of up to 40 years. Previous wet pre-storage of 5 to 7 years is considered to be realistic and feasible since nuclear power stations with compact storage racks can accommodate the spent fuel from 11 reloads and still have one full core reserve. However, shorter wet pre-storage periods as well might be of interest to some plants. The results reported above demonstrate that, depending on the given fuel assembly design, the fuel rod cladding material and the fuel assembly inservice power history, even more challenging conditions are possible at begin of storage. If very conservative umbrella conditions with their inherent conservative approaches violate licensing-related safety criteria, individual and more sophisticated dry storage performance assessments with a less conservative model approach will verify that more challenging begin-of-storage conditions remain within the licensed limits [20].

7. Conclusions

Licensing of dry storage casks requires that the spent LWR fuel stored does not develop systematic defects in the course of storage. The leading defect mechanism of LWR fuel with Zircaloy cladding is tangential creep due to fuel rod internal fission gas overpressure arising under dry storage conditions. Post-pile creep of Zircaloy is conservatively described by the creep of unirradiated material.

To comply with the requirements of extended burnup, Zircaloy-type cladding were developed within the allowed limits of Zircaloy specifications to achieve better corrosion resistance. The creep database for standard Zircaloy was therefore no longer adequate to sufficiently describe the improved cladding. A creep investigation program was performed for 6 different current cladding types with the view of supporting CASTOR V cask licensing for fuel assembly burnup of approximately 55 GWd/tHM. The test matrix embraced hoop stresses ranging from 80 to 150 N/mm^2 and test temperatures from 250 to 400°C. The tests lasted up to 10000 h.

From the test results yielded, the material displaying the fastest creep rate was as a basis for developing a mathematical approach to describing the creep in relation to stress, temperature and time. The selected interpolation formula slightly overestimates all test results.

In order to calculate the total creep strain of spent PWR fuel assemblies with a fuel rod burnup of 55 GWd/tHM containing uranium and MOX fuel, the end-of-life (EOL) conditions of such fuel with cladding displaying fast creep

and stronger cladding were calculated. The decay heat generates cask fuel rod hot spot temperatures between 348 and 357°C. The EOL fission gas release allows the determination of the hoop stress acting at the begin of storage taken into consideration as well the residual metallic wall thickness left from inservice corrosion of the fuel rod cladding.

The highest strain arising in a 40 year storage period in a CASTOR V/19 cask was 0.77%. This value is considerably lower than those values at which creep will adversely affect the Zircaloy-cladding of LWR spent fuel.

References

[1] Proc. IAEA Symp. on Safety and Engineering Aspects of Spent Fuel Storage, IAEA, Vienna, Austria, Oct. 10–14, 1994, foreword.

[2] A. Merkel, Rede der Bundesministerin für Umwelt, Naturschutz und Reaktorsicherheit, Jahrestagung Kerntechnik, May 1996, Mannheim.

[3] K. Janberg, 'Dry spent fuel storage in Germany: status and prospects', Proc. IAEA Symp. on Safety and Engineering Aspects of Spent Fuel Storage, IAEA, Vienna, Austria, Oct. 10–14, 1994, p. 307.

[4] M. Peehs, V. Dannert, M. Wickert, 'Interrelationship between design and end-of-life-conditions of spent fuel and back end of fuel cycle requirements, proceedings from storage in the nuclear fuel cycle', IMechE (Sept. 1996).

[5] R. Weh, D. Methling, M. Sappok, Zur Entsorgung deutscher Kernkraftwerke atw 41, 1996.

[6] M. Peehs, F. Takats, E. Vitkainen, K.M. Wasywich, 'The IAEA-coordinated research program on the behavior of spent fuel and storage facility components (BEFAST)', Proc. IAEA Symp. on Safety and Engineering Aspects of Spent Fuel Storage, IAEA, Vienna, Austria, Oct. 10–14, 1994, p. 157.

[7] 'Further analysis of extended storage of spent fuel', Final Report of a Co-ordinated Research Programme on the Behaviour of Spent Fuel Assemblies During Extended Storage (BEFAST III) 1991–1996, IAEA Tec Doc-944, May 1997.

[8] K.M. Wasywich, J. Freire-Canosa, S.J. Naqvi, 'Canadian spent fuel storage experience', Proc. IAEA Symp. on Safety and Engineering Aspects of Spent Fuel Storage, IAEA, Vienna, Austria, Oct. 10–14, 1994, p. 41.

[9] H. Kuriyama, H. Kato, T. Nakijama, M. Hirose, H. Sakamatsu, 'Storage facility for BWR spent fuel using casks in Japan', Proc. IAEA Symp. on Safety and Engineering Aspects of Spent Fuel Storage, IAEA, Vienna, Austria, Oct. 10–14, 1994, p. 71

[10] V.V. Morozov, V.V. Spichev, N.S. Tikhonov, S.V. Shihkin, 'Spent fuel management in the Russian federation: state of the art and outlook to the future', Spent Fuel Management: Status and Prospects, IAEA TEC DOC-732, Vienna, 1994, p. 83.

[11] R. Dodds, 'Status report on spent fuel management in the UK', Spent Fuel Management: Status and Prospects, IAEA TEC DOC-732, Vienna, 1994, p. 115.

[12] W.J. Park, 'Spent fuel management in Korea: past, present and future', Spent Fuel Management: Status and Prospects, IAEA TEC DOC-732, Vienna, 1994, p. 63.

[13] C. Pescatore, M. Cowgill, 'Temperature limit determination for the inert dry storage of spent nuclear fuel', EPRI TR-1039-49 final report, May 1994.

[14] M. Peehs, J. Fleisch, J. Nucl. Mater. 137 (1986) 190.

[15] G. Kaspar, M. Peehs, E. Steinberg, 'Experimental investigation of post-pile creep of Zircaloy cladding tubes', Trans. act. 8. SMIRT Conference 1985, Brussels, p. 81.

[16] M. Peehs, G. Kaspar, E. Steinberg, 'Experimentally-based spent fuel dry storage performance criteria', Proc. 3rd Int. Conf. on Spent Fuel Storage Technology, Seattle 1986, p. S-316.

[17] M. Peehs, R. Bokelmann, J. Fleisch, 'Spent fuel dry storage performance in inert atmosphere', Proc. 3rd Int. Conf. on Spent Fuel Storage Technology, Seattle 1986, p. S-215.

[18] J. Fleisch, M. Peehs, 'Analysis of spent fuel behavior in dry storage cask demonstration in Germany', Proc. 3rd Int. Conf. on Spent Fuel Storage Technology, Seattle 1986, p. S-253.

[19] S. Timoshenko, Strength of Materials, Part II, 3rd Ed. (van Nostrand, Princeton, NJ, 1956).

[20] V. Dannert, M. Peehs, W.D. Perschmann, Entsorgung moderner, betriebsoptimierter LWR-BE, Jahrestagung Kerntechnik, Mannheim, May 1996.